ANALYSIS OF NARROW EFFECTS IN $\bar{P}P$ ANNIHILATIONS

C. Defoix
Laboratoire de Physique Nucléaire du Collège de France - Paris.

1. INTRODUCTION

Putting aside the question of more "classic" resonances such η^0 and X°..., the narrow effects of interest are observed generally through rather high-multiplicity meson final states. According to the number of like particles forming these final states, one can distinguish two circumstances.

1) If this number is rather low, the number of particle combinations of a given type is limited, for instance from 1 to 4. Such is the case of the non-strange narrow effects which are observed in $\bar{p}p \to K\bar{K}n\pi$ (n=3 to 5) at 5.7 GeV/c [1]. These effects are detected in the $(K\bar{K}\pi)°$ and $(K\bar{K}\pi\pi)°$ mass distributions (Fig.1) at respectively 2.36 and 2.62 GeV/c^2 near the U^- and X^- positions. Neither cuts nor special selection methods are used.

2) The situation becomes different from the first if the number of like particles is such that the number of indistinguishable combinations is great. Such is the case if one has to analyze the (7π) final state, $\bar{p}p \to \pi^+\pi^+\pi^+\pi^-\pi^-\pi^-\pi°$. (nine $(\pi^+\pi^-\pi^0)$ combinations, 18 $(\pi^\pm\pi^\pm\pi^\mp\pi^0)$ combinations etc... per event).

Now, at low antiproton energy, this reaction has been analyzed to look for the possibility of cascading decays of the D° and E° mesons, through narrow $\eta^0\pi$ effects near the $K\bar{K}$-threshold mass, for instance [2]. Furthermore, observation of effects associated with such channels are complicated by reflections coming from another channel.

In the following, we shall describe briefly some methods of analysis that final states of this type require. A first method consists of separating two competing channels to minimize the reflections due to the undesirable one. Later techniques of analysis lead to the isolation of the only channel of interest and circumvent the problems of background and reflections due to irrelevant final states. Generally, all these processes are based on the presence of a narrow and identified resonance, for example the η^0 or $\omega^0(\to\pi^+\pi^-\pi^0)$. To be efficient, it is necessary that the observed width of such a basic resonance not be increased too much by experimental errors.

2. PROBLEMS MET IN THE DETECTION OF THE POSSIBLE $\delta\pi$ DECAY OF THE D°

The first evidence for a cascade decay of the D° was observed in $\bar{p}p$ annihilations into 7π at 1.2 GeV/c via the process [3] :

$$\bar{p}p \to D^\circ \pi^+ \pi^-$$
$$\hookrightarrow \delta^\pm \pi^\mp$$
$$\hookrightarrow \eta^0 \pi^\pm$$
$$\hookrightarrow \pi^+ \pi^- \pi^0$$

One can see in Fig.2 the "η^0"$\pi^\pm$ and "η^0"$\pi^+\pi^-$ mass distributions obtained from a $(\pi^+\pi^-\pi^0)$ selection at the η^0 mass. A narrow signal is observed at 975 MeV in $\eta^0\pi$ ($\Gamma \simeq 20$ MeV) and a bump at the D° mass in $\eta\pi\pi$ (M=1310 MeV; Γ = 40 MeV). These two signals are strongly correlated : The $\eta\pi$ signal is found again in the $\eta^0\pi^+\pi^-$ combinations selected in the D° region (1310 ± 30 MeV); furthermore the mass distribution of $\eta\pi\pi$ having at least one $\eta\pi$ combination in the δ region (975 ± 20 MeV) gives back the D° signal. However the (7π) final state is dominated by ω^0 production (about 70% - Fig.3). Unfortunately, because of this strong ω^0 production, an η^0 selection results in an ω^0 reflection in the $\eta\pi$ distribution in the neighborhood of the δ-mass. This reflection can be faked by a Monte-Carlo method (the result of such a simulation is shown in Fig.2) and does not explain either the narrow width of the signals nor the very localized correlation between the D°, $\delta^\pm$ and η^0 regions. Nevertheless, one can never be sure that such a Monte-Carlo description is sufficiently realistic, given the complexity of the (7π) final-state.

On the other hand, two other similar experiments simply add to the confusion : - at 1.1 GeV/c, in the 2-meter H.B.C. of CERN, where no distinction can be made between an ω^0 reflection and a genuine $\delta\pi$ effect[4];

- at 0.7 GeV/c in the 81-cm H.B.C.[5] for which the distributions are shown in Fig. 4 : the $\eta^0\pi^+\pi^-$ mass distribution shows a possible bump in the D° region, but this is right on the top of the phase space. The $\eta^0\pi^\pm$ distribution is no more enlightening, showing a shoulder at the δ-mass, which is the location of the ω^0 reflection.

3. METHOD OF SEPARATING TWO COMPETING CHANNELS

To reduce the non-η^0 background and attempt to overcome the ambiguity, ω^0 reflection-$\delta\pi$ effect, a first possibility consists of separating the $\eta^0 4\pi$ channel from the dominating $\omega^0 4\pi$. Ideally, one would calculate the probability for each event to come from one or the other reaction. Actually, we know neither the structure of the complete matrix elements $\bar{p}p \to \omega^0 4\pi$ and $\eta^0 4\pi$, nor what are the other channels going into the (7π) final state. The available information comes from the decay properties of the two basic resonances, η^0 and ω^0 which characterize

each channel. Therefore, one possibility is to construct estimators [5] taking into account the Breit-Wigner form, the experimental resolution (for example supposing a gaussian spread due to the errors) and the decay matrix element λ^{α} of both resonances ($\alpha = \eta^0$ or ω^0). By using these elements, the probability p^{α} for the n^{th} ($\pi^+\pi^-\pi^0$) combination (with an effective mass m_i) in one event to be an example of the resonance α can be deduced from the couple of measured variables (m_i, λ_i^{α}). The estimator which has been chosen is : $P_{\alpha} = \sum_{i=1,9} p_i^{\alpha}\ (m_i,\ \lambda_i^{\alpha})$

Each event corresponds to a point in the (P_{η^0}, P_{ω^0}) plane (Fig.5). By using as criteria the attenuation of the ω^0 signal and the enhancement of the $\eta^0 4\pi$ channel we find an optimal selection. The efficiency of the method is checked by a Monte-Carlo generation of the probability distribution of various (7π) final-states in the (P_{η^0}; P_{ω^0}) plane. The $\eta^0 4\pi$ channel is found to be enhanced by a factor 4 as compared with the other channels, and only 3% of all the ω^0 remain in the sample. The Fig.6 shows the results of the selection. A D°-$\delta^{\pm}$ correlation is found again. D° is found narrow (28 MeV for an experimental resolution equal to 12 MeV). In addition there is some indication of an $\eta^0\pi^+\pi^-$ and $\delta\pi$ decay of another object near 1400 MeV (G-parity equal to 1), which may be the E°.

4. METHOD TO LOCALIZE CHAINS OF DECAY THROUGH SUCCESSIVE NARROW OBJECTS

If the chain involves a well-identified narrow resonance or leads to such an object, one can proceed by displaying all the possible combinations of cascades as follows. For instance, if we are interested by cascading decays leading to the η^0, such as the D° or E°, we can consider all the cascades included in the different $\pi^+\pi^+\pi^0\pi^-\pi^-$ combinations by drawing a plane whose axes denote the mass of the $(5\pi)^\circ$ combinations and the mass of each $\pi^+\pi^+\pi^-\pi^0$ (and c.c.) combination contained in the $(5\pi)^\circ$; the two ($\pi^+\pi^-\pi^0$) combinations included in this $(4\pi)^{\pm}$ group are associated with each $(5\pi)^\circ$ - $(4\pi)^{\pm}$ pair $\{(3\pi)^\circ \subset (4\pi)^{\pm} \subset (5\pi)^\circ\}$.

The $\{(4\pi)^{\pm}$ - $(5\pi)^\circ\}$ mass-plane correlated kinematically with the η^0 region is divided into sections (100 in the present case), each corresponding to a range of $(5\pi)^\circ$ and $(4\pi)^{\pm}$ masses, and the mass distributions of the two $(3\pi)^\circ$ combinations for all points in each section are histogrammed. The most significant sections of such a display are shown in Fig.7 for the $\bar{p}p \to 7\pi$ analysis at 0.7 GeV/c [5]. The η^0 signal is spread out over all the squares, usually with a significance of less

than 3 s.d. in each one - except in one square shown in the center of the figure (square k - 6 s.d.), at the (D° - $\delta^\pm$) coordinates. So, a clear and narrow correlation is observed between the $(5\pi)^\circ$ combinations in the D° region, the included $(4\pi)^\pm$ combinations near the δ mass and the η^0 production. A less significant correlation can be seen in the square c between the E° - $\delta^\pm$ - η^0 regions as compared with the nearby squares.

One notices that this procedure circumvents the possibility of reflection coming from other channels, particularly the reflection of the ω^0 which is not contained in the field of observation.

5. ISOLATION OF THE CHANNEL OF INTEREST FROM A SAMPLE WITH REDUCTION OF THE NUMBER OF BODIES IN THE FINAL STATE.

Furthermore, one can project from the squares onto the $(5\pi)^\circ$ axes all the η^0-signals previously estimated above their respective backgrounds. One thus obtains the "true $\eta^0\pi^+\pi^-$ " mass distribution. Similarly, the projection onto the $(4\pi)^\pm$ axis gives the "true η^0 $\pi^\pm$" mass distribution. If we limit ourselves to the evolution of the η^0 signal in the D° band, we get the "true $\eta^0\pi^\pm$" distribution in D° etc...(Fig. 8). Obviously it is not necessary to pass by such a projection from the display to construct the $\eta\pi$ or $\eta\pi\pi$ mass distributions. These last and all others - (for instance for $\pi^+\pi^-$, $\pi^+\pi^+\pi^-\pi^-$, $\rho^0\pi^+\pi^-$ etc. recoiling against the η^0) can be deduced in a straightforward way by measuring the η^0-signal evolution versus the successive ranges of their mass values.

This method seems relevant to the analysis of the $\omega^0 4\pi$ channel in the (7π) sample. In fact, Figure 3 shows that there are about 4 indistinguishable $(3\pi)^\circ$ combinations for 1 "true ω^0" in the ω^0 mass range. An ordinary selection of these combinations to construct the "ω^0"$\pi^\pm$, "ω^0"$\pi^+\pi^-$ etc... mass distributions results in a strong non - ω^0 background which overwhelms the effects associated with the ω^0 production. Therefore the analysis of this channel by measuring the evolution of the ω^0 signal versus the different multipion effective masses(or angular emission), circumvents the problem of selection of the "true ω^0" combination. At the same time, the (7π) analysis is reduced to a five-body problem, and, except for the statistical fluctuations, such a manner of selecting the $\omega^0 4\pi$ channel from the sample does not bring with it events of the non-ω^0 channel. Finally the channel of interest is selected in its entirety.

The eventual bias of the method can be controlled by adding to the study of variation of the ω^0 signal in the $(3\pi)^\circ$ mass distribution, that of the decay matrix element λ_{ω^0} in the ω^0 mass range [6].

The analysis of this channel at 0.7 and 1.2 GeV/c by means of this method leads to evidence for a narrow effect (6.s.d.) in the $\omega^0\pi^\pm$ mass distribution near 1050 MeV, shown in Fig.9b for $\bar{p}p$ annihilations at 700 MeV/c (Γ = 30 MeV for an experimental resolution equal to about 15 MeV). This last enhancement was also observed by using several simpler methods of background subtraction [6]. However, given the loss of statistics these methods involve, this observation was less significant (Fig. 9a). This study is not ended, but this effect seems to be correlated with an $\omega^0\pi^+\pi^-$ enhancement centered at 1.33 GeV ($\Gamma \simeq$ 50 MeV). Since all that corresponds to the G-parity and usual mass and width of the A_2 observed in the $\bar{p}p$ annihilation through its $\rho\pi$ and $\eta\pi$ decay modes, maybe an interpretation of this effect is possible in terms of a new A_2 decay.

REFERENCES

1) H.W. Atherton et al., Evidence for narrow non-strange neutral bosons of masses 2.37 and 2.61 GeV produced in $\bar{p}p$ annihilations at 5.7 GeV/c, CERN/D.Ph II/Phys 71-18 (1971).

2) A. Astier et al., Further study of the I=1 $K\bar{K}$ structure near threshold, Physics Letters, vol.25B,n° 4 (1967).

Ch. d'Andlau et al., Analysis of the I=O ($K\bar{K}\pi$) resonances produced in $\bar{p}p$ annihilations at O,7 GeV/c : the D, E and f' mesons, Nuclear Physics, B14, 63 (1969).

3) C. Defoix et al., Evidence for the existence of a narrow $\eta^0\pi^\pm$ resonance at 975 MeV, interpreted as a decay of the $\delta^\pm$ meson, and evidence for a $\delta^\pm\pi$ decay of the D° meson, Physics Letters 28B, p. 353 (1968).

4) R.A. Donald et al., Search for D° and $\delta^\pm$ (962) mesons in $\bar{p}p \to 3\pi^+3\pi^-\pi^0$ XVth International Conference on High Energy Physics - KIEV (1970)

5) C. Defoix et al., Evidence for decays of the D and E mesons into $\delta\pi$ in $\bar{p}p$ annihilations at 700 MeV/c. Submitted to Nuclear Physics B.

6) C. Defoix et al., Resonance production in the $\bar{p}p \to \omega^0 2\pi^+ 2\pi^-$ annihilations at 0.7 and 1.2 GeV/c. Proceedings of the XVth International Conference on Elementary Particles - KIEV (1970).

FIGURE CAPTIONS

Fig. 1) Distribution of neutral $K\bar{K}\pi\pi$ and $K\bar{K}\pi$ masses from the following $\bar{p}p$ final states at 5.7 GeV/c [1] : a) $\bar{p}p \to K_1^o(K^o)2\pi^+2\pi^-$
$\to K_1^o\, K^{\pm}\pi^{\mp}\pi^+\pi^-$
b) $\bar{p}p \to K^{\pm}\, K^o\pi^{\mp}\pi^+\pi^-\pi^0$
$\to K_1^o\, K_1^o\, 2\pi^+2\pi^-$

Fig. 2) Distributions of $\eta^0\pi^{\pm}$ and $\eta^0\pi^+\pi^-$ masses from $\bar{p}p \to 3\pi^+3\pi^-\pi^0$ at 1.2 GeV/c.

Fig. 3) Distributions of $\pi^+\pi^-\pi^0$ mass and $\lambda\omega$ from $\bar{p}p \to 3\pi^+3\pi^-\pi^0$ at (a) 0.7 GeV/c and (b) 1.2 GeV/c.

Fig. 4) Distribution of $\eta^0\pi^{\pm}$ and $\eta^0\pi^+\pi^-$ masses from $\bar{p}p \to 3\pi^+3\pi^-\pi^0$ at 0.7 GeV/c.

Fig. 5) Distribution of $(P_{\eta^0}, P_{\omega^0})$ pairs from $\bar{p}p \to 7\pi$ at 0.7 GeV/c.

Fig. 6) From the reaction $\bar{p}p \to 7\pi$ at 0.7 GeV/c, distributions of the following mass combinations using $(P_{\eta^0}, P_{\omega^0})$ selection method:
(a) $\eta^0\pi^+\pi^-$,
(b) $\delta^{\pm}\pi^{\mp}$
(c) $\eta^0\pi^{\pm}$
(d) $\eta^0\pi^{\pm}$ from $\eta^0\pi^+\pi^-$ in D° region,
(e) $\eta^0\pi^{\pm}$ from $\eta^0\pi^+\pi^-$ in E° region.

Fig. 7) Display of $\pi^+\pi^-\pi^0$ mass combinations, in $\bar{p}p \to 7\pi$ at 0.7 GeV/c, associated with $(4\pi)^{\pm}$ and $(5\pi)°$ masses such that $(3\pi)° \subset (4\pi)^{\pm} \subset (5\pi)°$; $(5\pi)°$ and $(4\pi)^{\pm}$ mass ranges are indicated, respectively, at left and above the display; $(3\pi)^o$ mass and number of combinations, below and at right.

Fig. 8) Distributions of $\eta^0\pi(\pi)$ masses from $\bar{p}p \to 7\pi$ at 0.7 GeV/c made by counting the number of η^0 above background for each $\eta^0\pi(\pi)$- mass division
(a) Total $\eta^0\pi^{\pm}$
(b) $\eta^0\pi^{\pm}$ contained in $(5\pi)°$ in the D° band.
(c) $\eta^0\pi^{\pm}$ contained in $(5\pi)°$ in the E° band.
(d) Total $\eta^0\pi^+\pi^-$.

Fig. 9) Distributions of $\omega^0\pi^{\pm}$ masses from $\bar{p}p \to \omega^0\pi^+\pi^+\pi^-\pi^-$ at 0.7 GeV/c.
(a) Various background-selection methods used.
(b) Distribution generated by counting events in ω^0 signal above background.

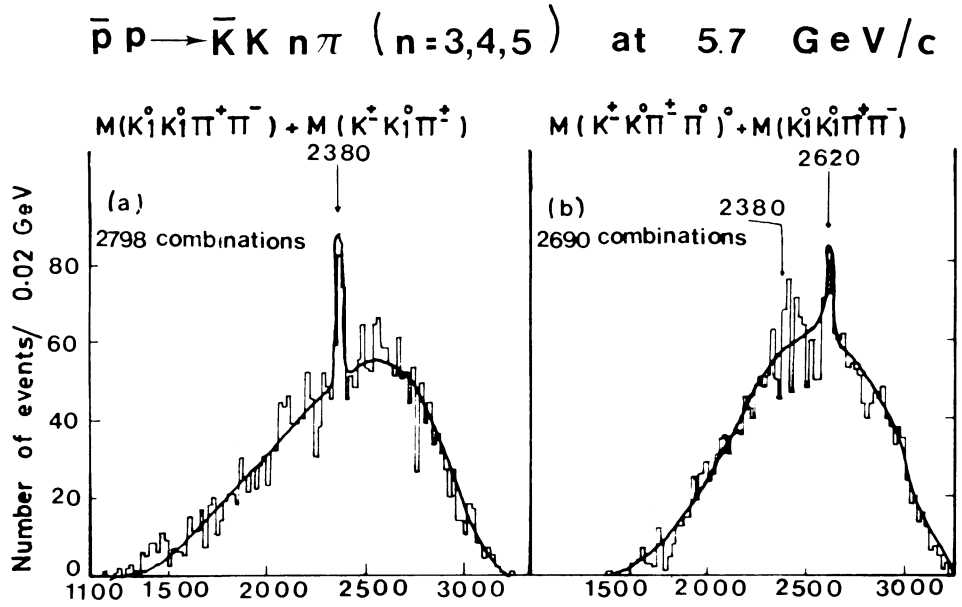
$\bar{p}p \rightarrow \bar{K}K\,n\pi$ (n=3,4,5) at 5.7 GeV/c
M(K°iK°iπ⁺π⁻) + M(K⁺K°iπ⁺)
M(K⁺K°π±π°)° + M(K°iK°iπ⁺π⁻)
2380
2620
(a)
2798 combinations
(b)
2690 combinations
Number of events/ 0.02 GeV
0
20
40
60
80
1100 1500 2000 2500 3000
1500 2000 2500 3000

Fig. 1

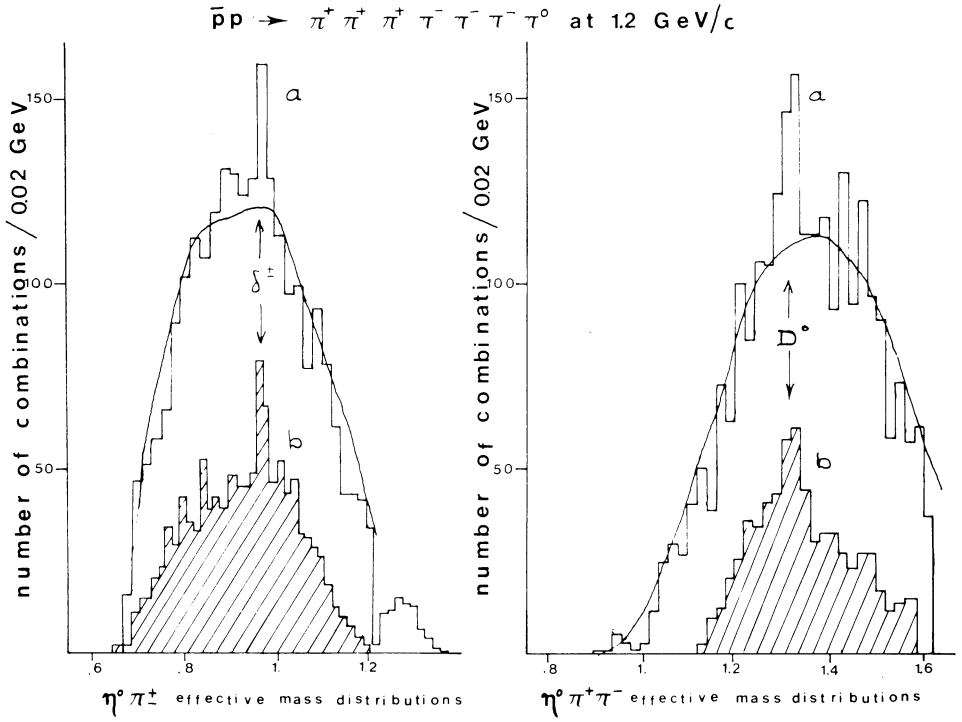
$\bar{p}p \rightarrow \pi^+\pi^+\pi^+\pi^-\pi^-\pi^-\pi^\circ$ at 1.2 GeV/c
number of combinations /0.02 GeV
50
100
150
a
b
$\delta^\pm$
D°
.6
.8
1.
1.2
1.4
1.6
$\eta^\circ\pi^\pm$ effective mass distributions
$\eta^\circ\pi^+\pi^-$ effective mass distributions

Fig. 2

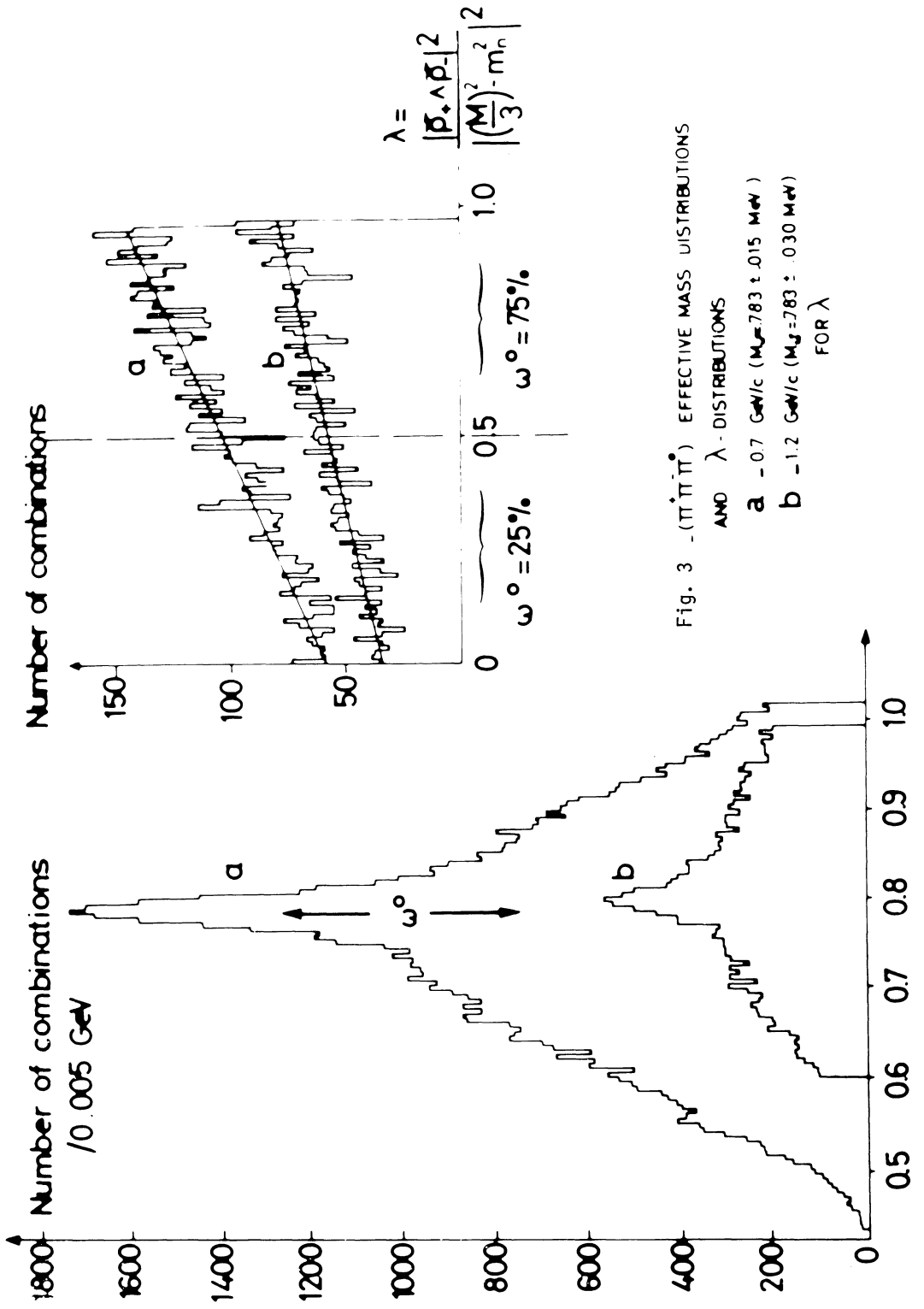

Fig. 3 $-(\pi^+\pi^-\pi^0)$ EFFECTIVE MASS DISTRIBUTIONS AND λ - DISTRIBUTIONS

a -0.7 GeV/c ($M_\omega = 783 \pm 015$ MeV)

b -1.2 GeV/c ($M_\omega = 783 \pm 030$ MeV) FOR λ

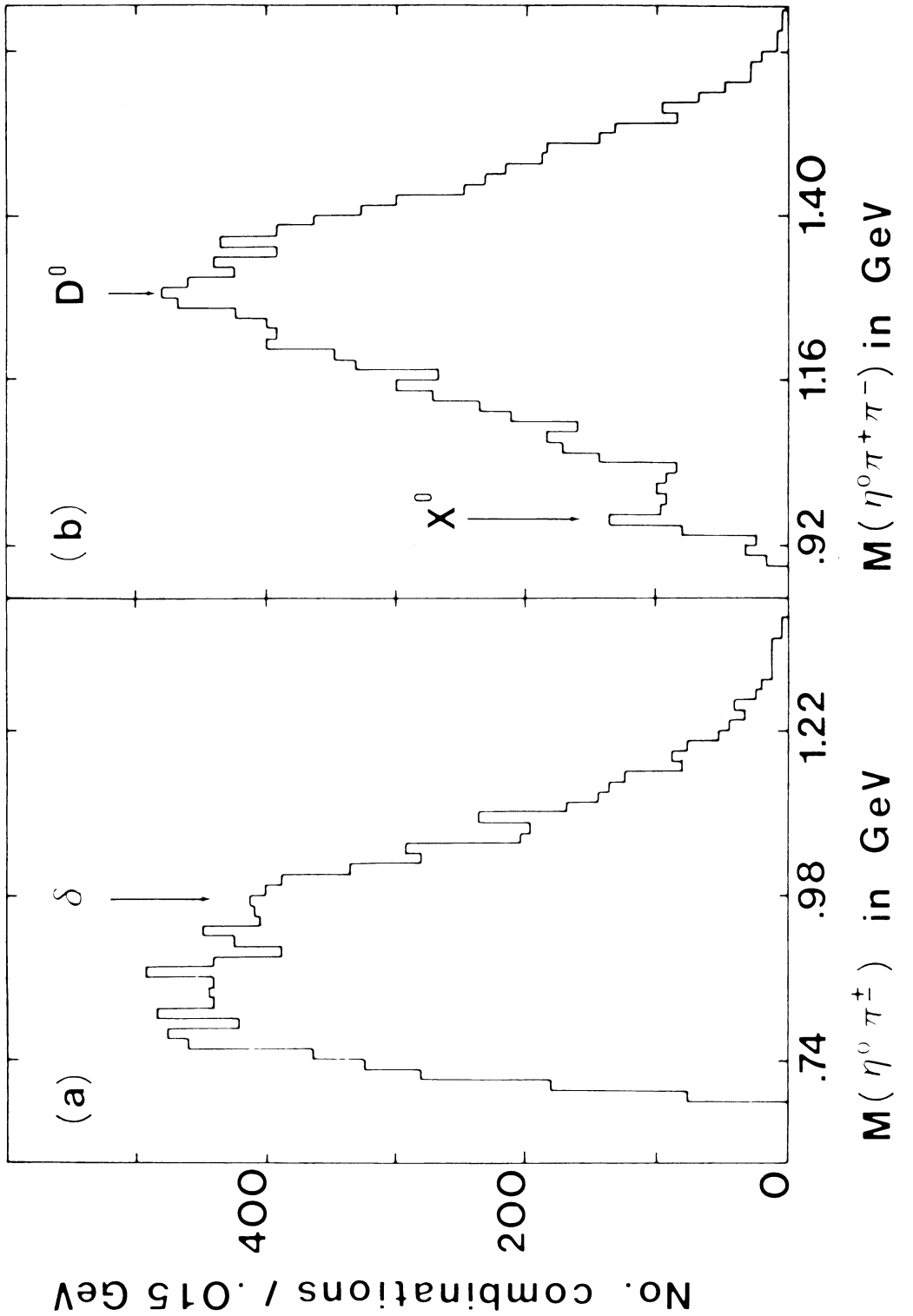
No. combinations / .015 GeV
400
200
0
(a)
δ
(b)
D⁰
X⁰
.74
.98
1.22
.92
1.16
1.40
M(η⁰ π±) in GeV
M(η⁰π⁺π⁻) in GeV

Fig. 4

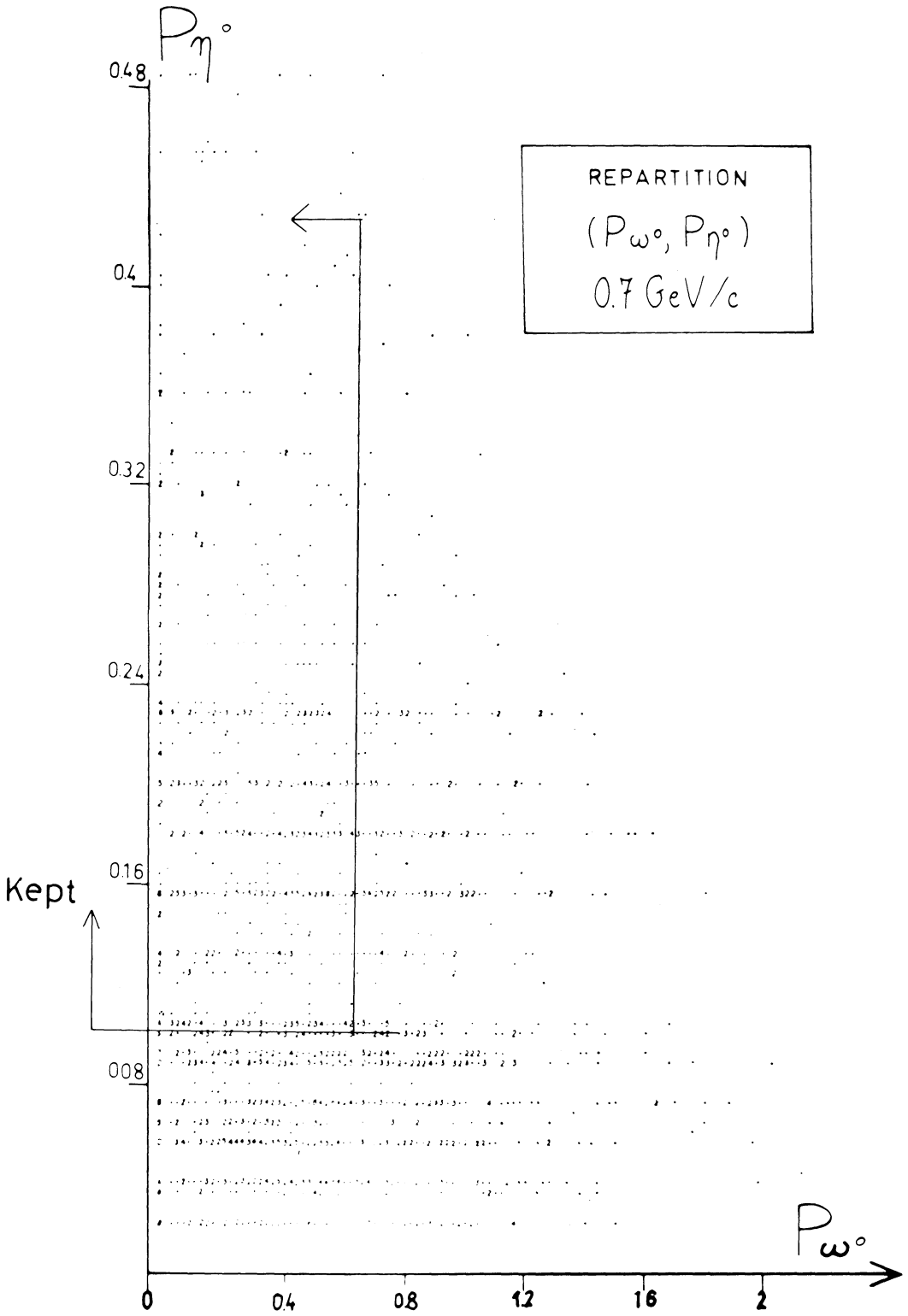
P_{η°
0.48
0.4
0.32
0.24
0.16
0.08
Kept
REPARTITION
$(P_{\omega^\circ}, P_{\eta^\circ})$
0.7 GeV/c
P_{ω°
0
0.4
0.8
1.2
1.6
2

Fig. 5

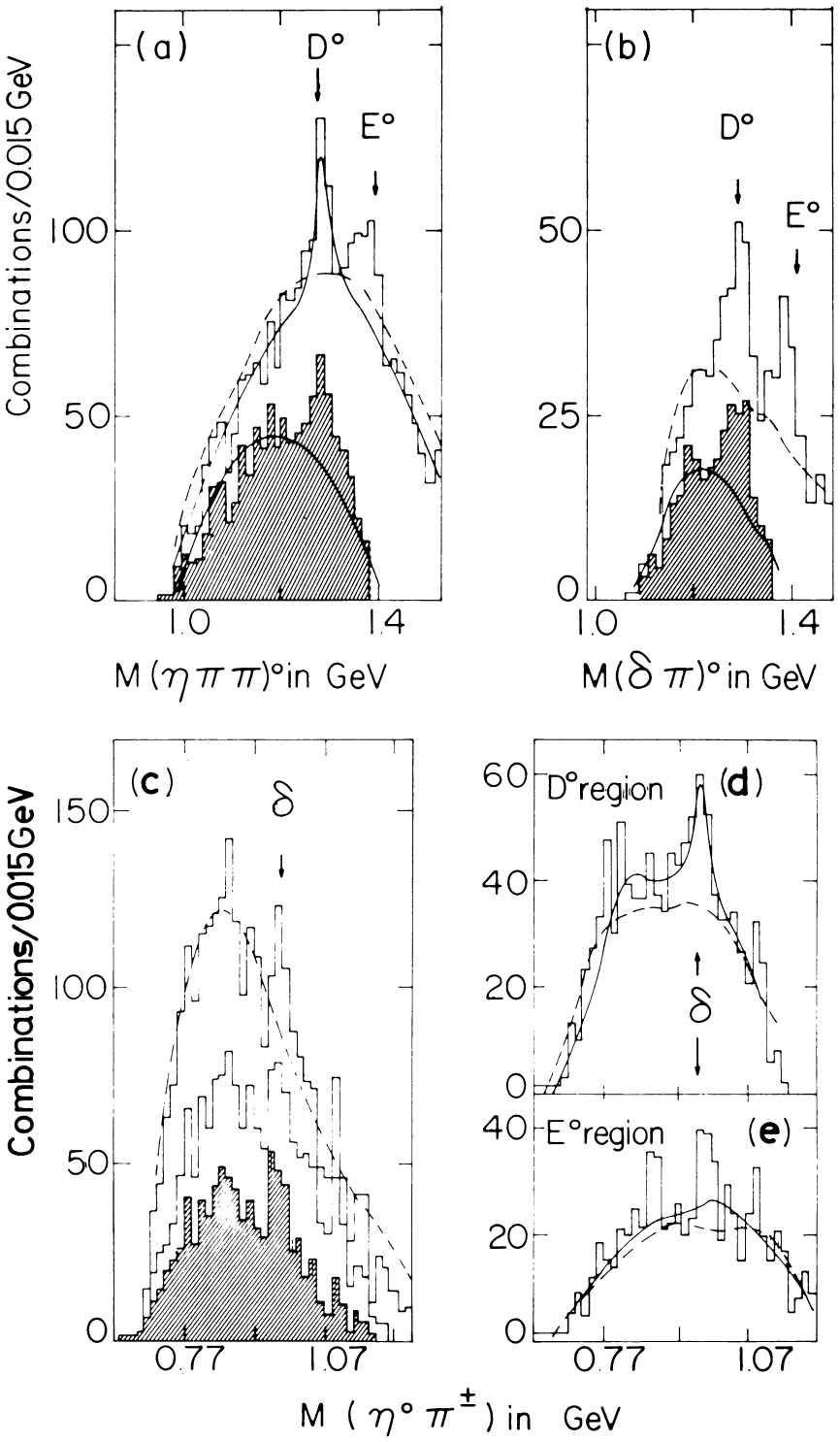
(a)
D°
E°
(b)
D°
E°
Combinations/0.015 GeV
100
50
0
1.0
1.4
M (η π π)° in GeV
50
25
0
1.0
1.4
M (δ π)° in GeV
(c)
δ
Combinations/0.015 GeV
150
100
50
0
0.77
1.07
D°region
(d)
60
40
20
0
δ
E°region
(e)
40
20
0
0.77
1.07
M (η° π±) in GeV

Fig. 6

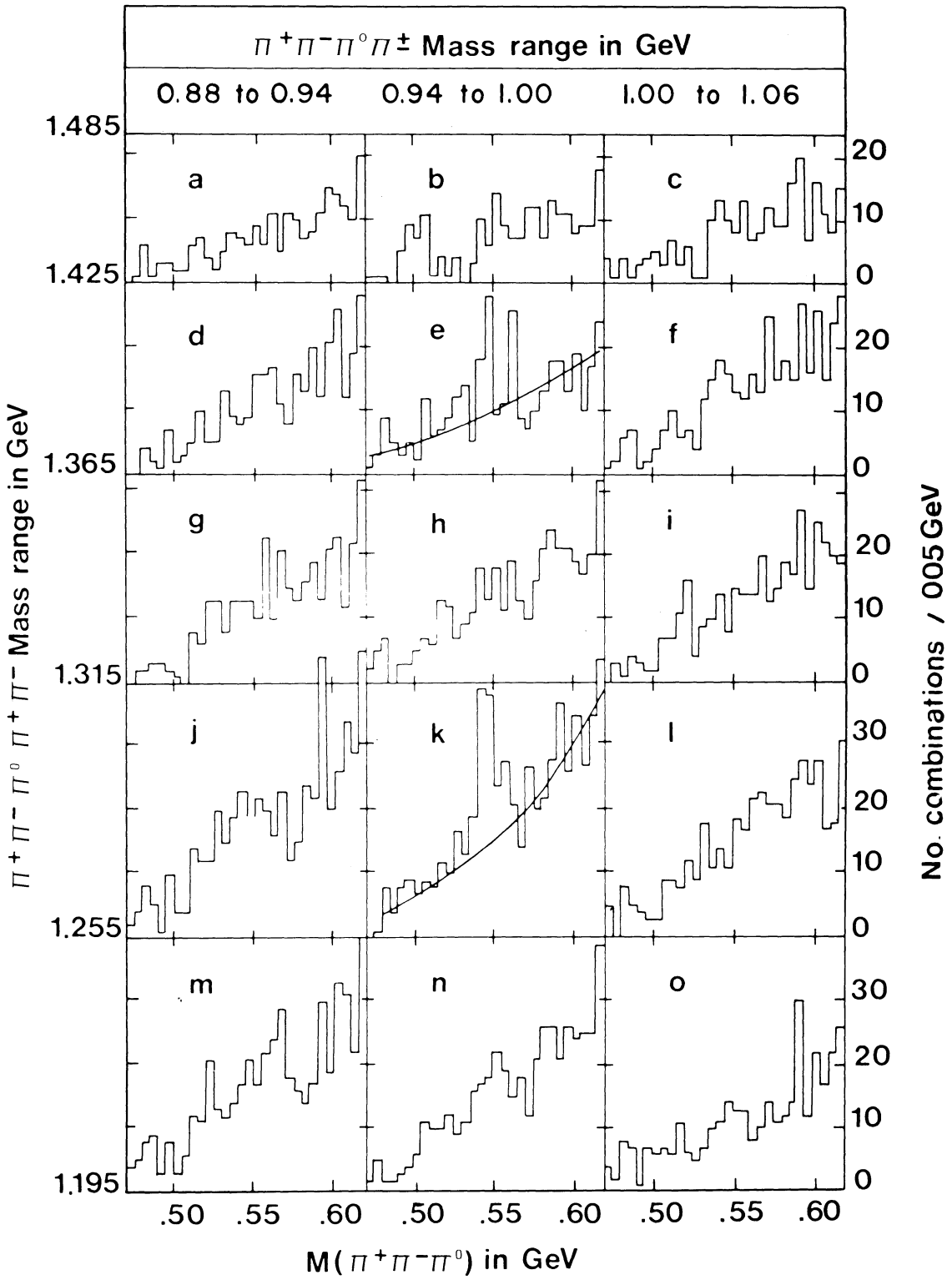
$\pi^+\pi^-\pi^0\pi^\pm$ Mass range in GeV
0.88 to 0.94
0.94 to 1.00
1.00 to 1.06
1.485
1.425
1.365
1.315
1.255
1.195
a
b
c
d
e
f
g
h
i
j
k
l
m
n
o
20
10
0
30
.50
.55
.60
$\pi^+\pi^-\pi^0\pi^+\pi^-$ Mass range in GeV
No. combinations / 005 GeV
M($\pi^+\pi^-\pi^0$) in GeV

Fig. 7

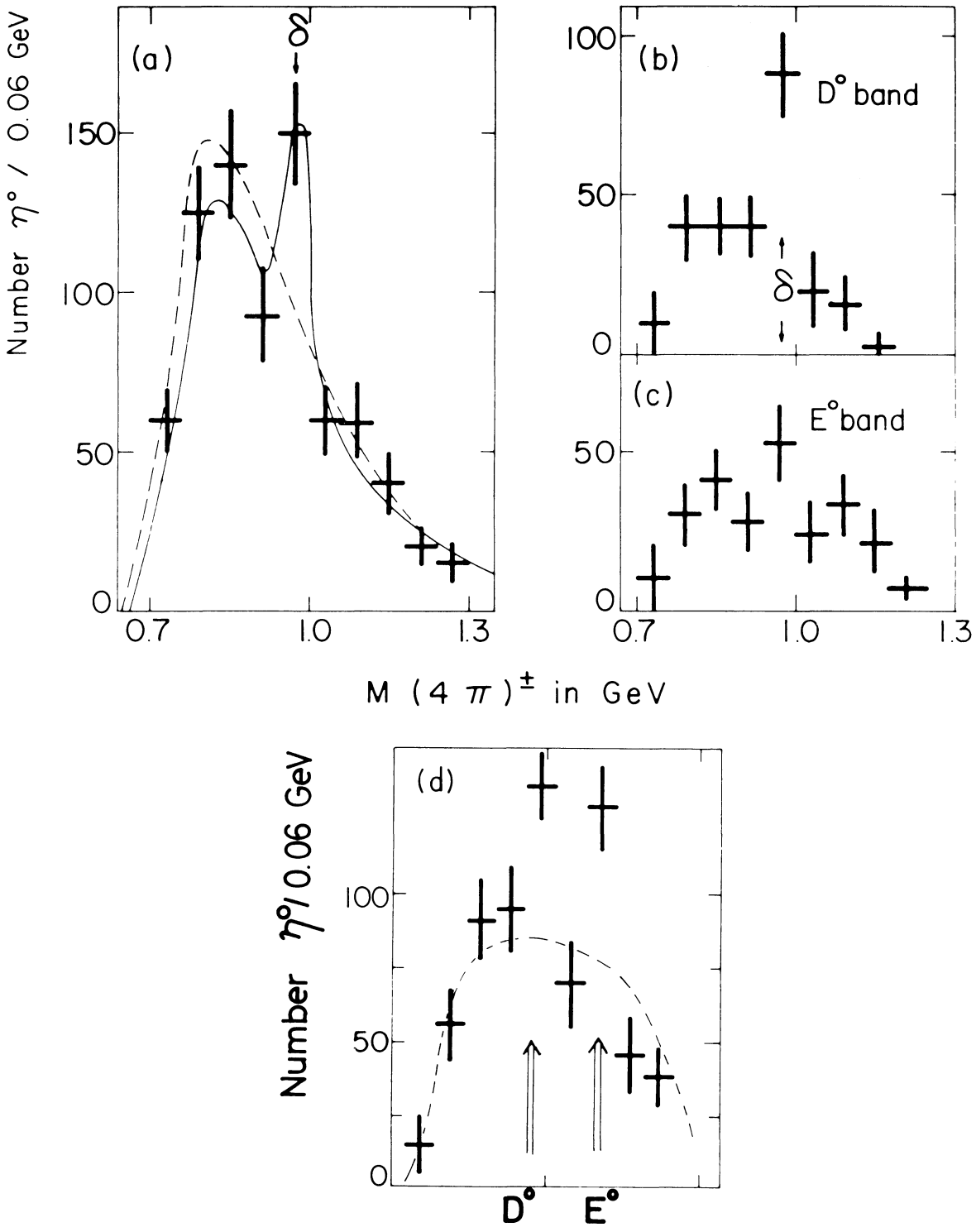
(a)
(b)
D° band
(c)
E° band
(d)
Number η° / 0.06 GeV
M (4π)± in GeV
Number η°/0.06 GeV
D°
E°

Fig. 8

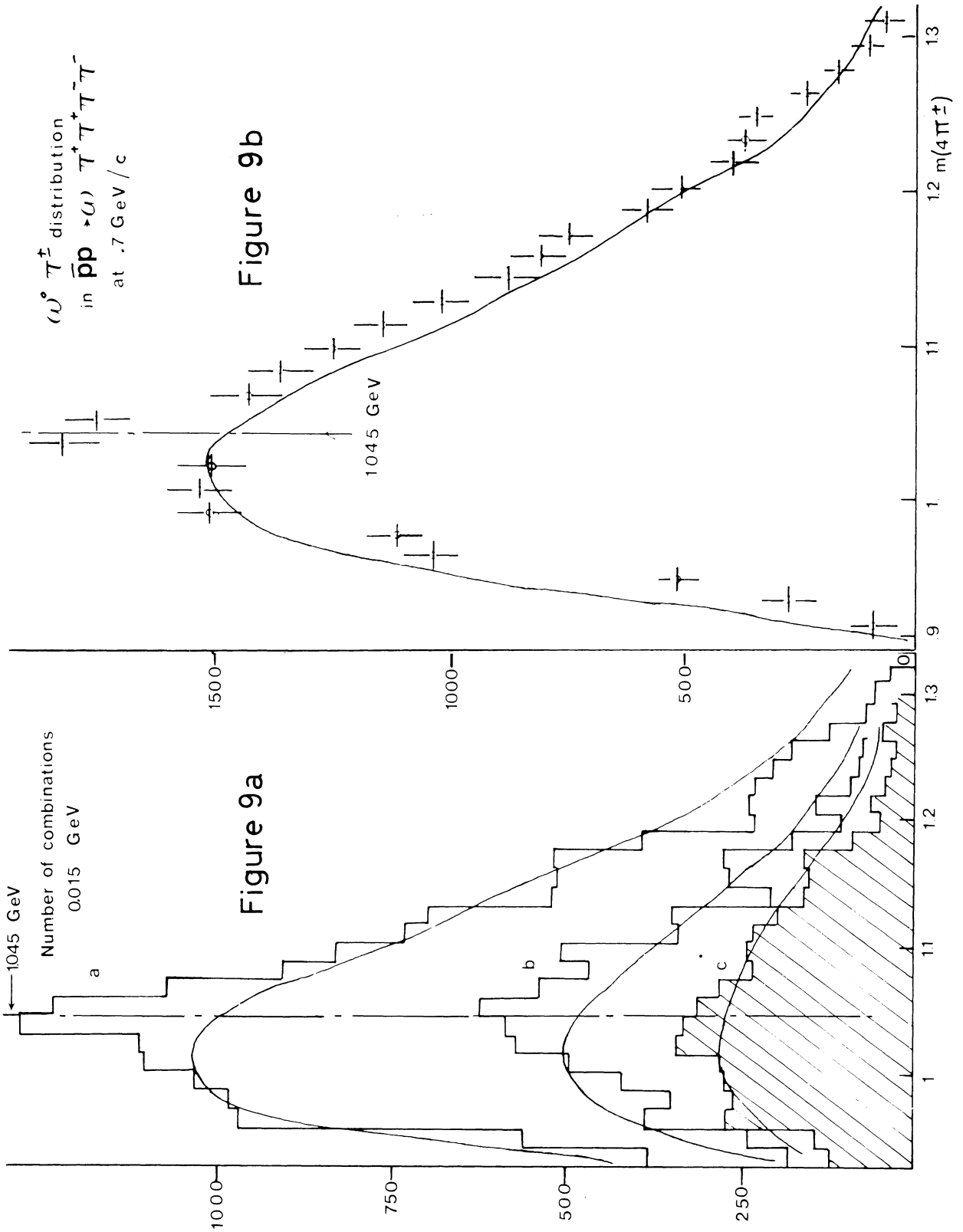
Figure 9a
1045 GeV
Number of combinations
0.015 GeV
a
b
c
1000
750
500
250
1500
1000
500
1
1.1
1.2
1.3
Figure 9b
$\omega^0 \pi^\pm$ distribution
in $\bar{p}p \to \omega\, \pi^+\pi^+\pi^-\pi^-$
at .7 GeV/c
1045 GeV
.9
1
1.1
1.2 m(4π±)
1.3

Fig. 9a

Fig. 9b

DISCUSSION AND COMMENTS

Mr. Donald : Since we learned about Defoix's method of displaying the data, we have looked at the same distributions. We tend to find η for every selection of 5π mass and 4π mass, we have examined so far. The interpretation is not clear, but the effect $D \to \delta\pi \to \eta\pi\pi$ is not nearly so strong as Defoix apparently sees at 700 MeV/c.